

## Surfactant Control of Gas Transport and Reactions at the Surface of Sulfuric Acid

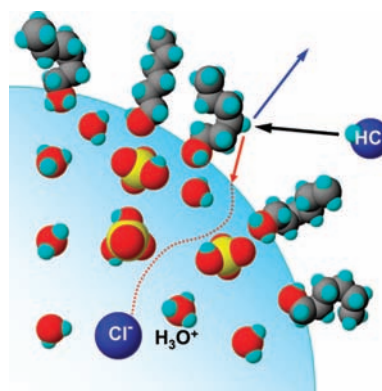
SEONG-CHAN PARK, DANIEL K. BURDEN, AND  
GILBERT M. NATHANSON\*

*Department of Chemistry, University of Wisconsin—Madison, 1101 University Avenue, Madison, Wisconsin 53706*

RECEIVED ON AUGUST 1, 2008

### CON SPECTUS

**A**erosol particles in the atmosphere are tiny chemical reactors that catalyze numerous reactions, including the conversion of benign gases into ozone-destroying ones. In the lower stratosphere, these particles are often supercooled mixtures of water and sulfuric acid. The different species present at the surface of these droplets ( $\text{H}_2\text{O}$ ,  $\text{H}_3\text{O}^+$ ,  $\text{HSO}_4^-$ ,  $\text{H}_2\text{SO}_4$ , and  $\text{SO}_4^{2-}$ ) stand at the “gas–liquid frontier”; as the first to be struck by impinging molecules, these species provide the initial environment for solvation and reaction. Furthermore, aerosol particles may contain a wide range of organic molecules, some of which migrate to the surface and coat the droplet. How do ambient gases dissolve in the droplet if it is coated with an organic layer? At one extreme, monolayer films of insoluble, long-chain alcohols can dramatically reduce gas transport, packing so tightly at the surface of water that they impede water evaporation by factors of 10 000 or more. Shorter chain surfactants are expected to pack less tightly, but we wondered whether these incomplete monolayers also block gas transport and whether this system could serve as a model for understanding the surfaces of atmospheric aerosol particles.



To address these questions, our research focuses on small, soluble surfactants such as butanol and hexanol dissolved in supercooled sulfuric acid. These amphiphilic molecules spontaneously segregate to the surface and coat the acid but only to a degree. Gas–liquid scattering experiments reveal that these porous films behave in surprisingly diverse ways: they can impose a barrier (to  $\text{N}_2\text{O}_5$  hydrolysis), be “invisible” (to water evaporation), or even enhance gas uptake (of HCl). The transition from obstacle to catalyst can be traced to specific interactions between the surfactant and each gas. For example, the hydrolysis of  $\text{N}_2\text{O}_5$  may be impeded because of its large size and because alcohol molecules that straddle the interface limit contact between  $\text{N}_2\text{O}_5$  and its  $\text{H}_3\text{O}^+$  and  $\text{H}_2\text{O}$  reaction partners. However, these same alcohol molecules assist HCl dissociation because the alcohol OH groups provide extra interfacial protonation sites. Interestingly, butanol does not impede water evaporation, in part because the butyl chains pack much more loosely than insoluble, long-chain surfactants. Through these investigations, we hope to gain insight into the mechanisms by which surfactants on sulfuric acid and other aqueous solutions affect transport and reactivity at the gas–liquid interface.

### Introduction: Monolayer Experiments To Try at Home

Surfactants (surface-active agents) behave in delightful ways on the surface of water.<sup>1–3</sup> To get a feeling for surfactant films, fill a dish with water, lightly sprinkle talc on the surface, and place a drop of dishwashing liquid at the center. The rapidly spreading talc indicates that the surfactant (such as sodium dodecylbenzenesulfonate) coats

the surface. You can even make talc “dance” on the surface by adding a volatile surfactant such as paint thinner (acetone). Next, fill two glasses to the brim with water and touch one surface with dishwashing liquid. After a few days, the glass with soapy water will be fuller because the soap film impedes water evaporation.

These experiments reveal features of surfactants that we explore herein to learn how soluble

organic molecules spread on sulfuric acid and alter gas transport and interfacial reactions.

## Reactions in Sulfuric Acid Aerosols

Many reactions in the atmosphere are mediated by submicrometer sulfuric acid droplets. These particles vary in composition from 40 to 80 wt %  $\text{H}_2\text{SO}_4$  at 240 to 200 K in the lower stratosphere but are less acidic in the upper troposphere due to absorption of  $\text{NH}_3$ .<sup>4–7</sup> The acid is produced in the stratosphere primarily from the oxidation of OCS originating in the ocean and  $\text{SO}_2$  emitted by volcanoes.<sup>6</sup> These droplets facilitate reactions of the benign gases HCl and HBr with HOCl, HOBr, ClONO<sub>2</sub>, and BrONO<sub>2</sub> to generate Cl<sub>2</sub>, Br<sub>2</sub>, and BrCl.<sup>7–9</sup> The halogen gases then evaporate from the droplets and photolyze into Cl and Br atoms that catalytically destroy ozone.<sup>10</sup> Sulfuric acid droplets also hydrolyze  $\text{N}_2\text{O}_5$  into  $\text{HNO}_3$ , effectively removing  $\text{NO}_2$  and  $\text{NO}_3$  from the atmosphere.<sup>7,10</sup> This removal suppresses the NO/NO<sub>2</sub>-catalyzed destruction of ozone but enhances the Cl/ClO cycle by curtailing conversion of reactive ClO into ClONO<sub>2</sub>.

Remarkably, field measurements indicate that aqueous droplets in the upper troposphere (and just into the stratosphere) contain significant amounts of organic matter.<sup>11,12</sup> Some of these species may accumulate at the surface of the droplet because they contain water-insoluble hydrocarbon chains attached to water-soluble groups such as OH and COOH;<sup>2,12–14</sup> this organic coating may then restrict gas transport across the surface.<sup>15–18</sup> In order for a surfactant film to impede gas–liquid reactions, however, gas entry into the droplet must be hampered enough to be rate-limiting. For the reaction  $\text{HCl}(\text{g}) + \text{HOBr}(\text{aq}) \rightarrow \text{BrCl}(\text{g}) + \text{H}_2\text{O}$  in 60 wt %  $\text{H}_2\text{SO}_4$  at 213 K, the HCl entry probability must drop below  $10^{-4}$  in order to limit the low rate of this bulk-phase reaction, which proceeds slowly because of the naturally low concentrations of HCl and HOBr in the acid droplets.<sup>19,20</sup> In contrast, the solute–solvent reaction  $\text{N}_2\text{O}_5(\text{g}) + \text{H}_2\text{O} \rightarrow 2\text{HNO}_3(\text{aq})$  occurs approximately once in every ten  $\text{N}_2\text{O}_5$  collisions with the acid droplet.<sup>5,21</sup> This higher probability places a smaller burden on the surfactant to impede reaction. Indeed, organic films have been postulated as one explanation for the variability in  $\text{N}_2\text{O}_5$  hydrolysis rates in aerosol particles over the northeast United States.<sup>22</sup>

## Surfactant Films on Sulfuric Acid

Can such reductions in interfacial gas transport be caused by surface-active molecules that exist in upper tropospheric aerosol particles? While the chemical speciation is not firmly established, there appears to be a wide variety of amphiphilic

molecules in the troposphere ranging from methanol to fatty acids that are generated by vegetation and microorganisms and more locally by aircraft exhaust.<sup>7,12,13,23,24</sup> Numerous experiments show that insoluble, long-chain surfactants such as hexadecanol ( $\text{C}_{16}\text{H}_{33}\text{OH}$ ) and stearic acid ( $\text{C}_{17}\text{H}_{35}\text{COOH}$ ) form compact monolayers on water that inhibit rates of water evaporation by  $10^4$  or more,<sup>15</sup> with resistances that grow exponentially with chain length.<sup>2,16,17,25</sup> These films also reduce the uptake of ammonia and water into room temperature sulfuric acid aerosols<sup>26</sup> and suppress the hydrolysis of  $\text{N}_2\text{O}_5$  up to 60-fold.<sup>27</sup> Kinks and branches in the alkyl chains and mixtures of surfactants moderate their resistance to gas transport substantially.<sup>28,29</sup>

Relatively little is known about the permeability of soluble, short-chain surfactants on water or sulfuric acid. Several studies indicate that slightly soluble  $\text{C}_8$ – $\text{C}_{12}$  alcohols in water can impede  $\text{H}_2\text{O}$  and  $\text{CO}_2$  transport.<sup>26</sup> Recent experiments show that monolayers of hexanoic acid<sup>30</sup> and sodium dodecyl sulfate<sup>31</sup> on seawater suppress  $\text{N}_2\text{O}_5$  hydrolysis by factors of 3 and 10, respectively, and that an octanol monolayer on water impedes the uptake of  $\text{HNO}_3$  and  $\text{NH}_3$  by 6- and 4-fold.<sup>32</sup> Conversely, organic films can enhance uptake when the gas is more soluble in the surface film than in the subphase, as shown by the adsorption of anthracene onto 1-octanol films on water.<sup>12,33</sup>

Our own studies utilize 1-butanol (BuOD) or 1-hexanol (HexOD) as model surfactants and 56–68 wt %  $\text{D}_2\text{SO}_4$  (0.20 to 0.30 mol fraction acid) at 213 K as the subphase acid in order to mimic the composition of stratospheric sulfuric acid droplets. The vapor pressures of these solutions lie below  $10^{-3}$  Torr,<sup>4</sup> which are low enough to perform gas–liquid scattering experiments.<sup>34</sup> The acid reacts with the alcohols to produce  $\text{ROD}_2^+$ , while the formation of  $\text{ROSO}_3\text{D}$  is slow and strongly suppressed at 213 K.<sup>35</sup> Alcohol protonation increases at higher acidities, and at 273 K, the ratio  $\text{ROD}_2^+/\text{ROD}$  rises from  $\sim 0.4:1$  to  $\sim 0.9:1$  in 56 and 68 wt %  $\text{D}_2\text{SO}_4$ , respectively.<sup>36</sup> Because the  $\text{ROD}_2^+$  ions repel each other at the surface, the alcohol films are less compact at higher acidities. According to our Gibbs adsorption analysis of surface tensions measured at 295 and 250 K and extrapolated to 213 K, the total saturated surface concentration of hexyl species (HexOD and  $\text{HexOD}_2^+$ ) corresponds to  $\sim 68\%$ ,  $\sim 66\%$ , and  $\sim 62\%$  of a compact film of all-trans chains for 56, 60, and 68 wt %  $\text{D}_2\text{SO}_4$ , respectively.<sup>37,38</sup> The shorter butanol chains assemble more loosely and reach  $\sim 50\%$  coverage on 60 wt % acid. Although hexanol packs more tightly than butanol, the hexyl chains possess more kinks because of their two additional  $\text{CH}_2$  groups.<sup>39</sup>

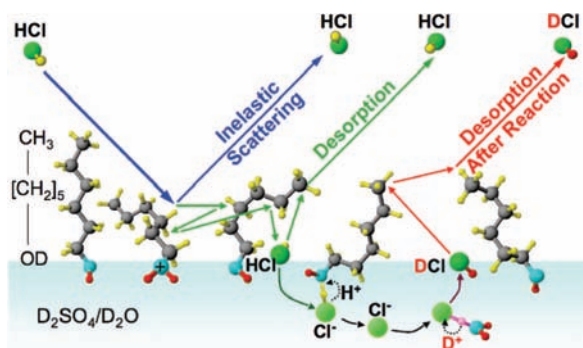


**FIGURE 1.** Pathways for HCl molecules colliding with liquid  $D_2SO_4/D_2O$  covered with 1-hexanol.

## Molecular Beam Scattering from Sulfuric Acid

We employ gas–liquid scattering experiments in order to investigate the effects of soluble surfactants on interfacial gas transport and reactions. This technique provides a way to disentangle the elementary steps in collisions and reactions involving a wide range of low vapor pressure liquids.<sup>40</sup> Figure 1 illustrates several pathways for an HCl molecule colliding with deuterated sulfuric acid coated with hexanol. The impinging HCl molecules may scatter directly from the surface in one or a few collisions, or they may dissipate their kinetic energy and become momentarily trapped (physisorbed) by attractive forces between HCl and surface species. These “frontier” species consist of  $D_2O$ ,  $D_3O^+$ ,  $DSO_4^-$ , and perhaps  $D_2SO_4$  and  $SO_4^{2-}$ ,<sup>9</sup> in addition to HexOD and  $HexOD_2^+$  that segregate to the surface. Some of the thermally equilibrated HCl are propelled back into vacuum by motions of the surface molecules, before or after penetrating between the hexyl chains, or even after contact with the acid itself. As pictured in Figure 1, other HCl molecules that reach the acid may form hydrogen bonds to interfacial OD groups and dissociate and dissolve,<sup>9</sup> ultimately desorbing as DCI after  $D \rightarrow H$  exchange. We characterize these pathways by monitoring HCl and DCI as they exit from the film-coated acid.

Figure 2 depicts the gas–liquid scattering apparatus.<sup>41</sup> A Teflon reservoir containing the acid is first situated inside the vacuum chamber. The solution is then doped with 1-butanol (0–1 M) or 1-hexanol (0–0.1 M) and cooled to 213 K. A continuously renewed, vertical acid film is formed by rotating a glass wheel partially submerged in the acid solution. The outer portion of the film is skimmed away by a Teflon scraper, and the remaining  $\sim 0.03$  cm thick layer passes in front of a hole in the reservoir, where it is exposed to the impinging HCl beam. The time between scraping and exposure is typically 1 s, which is long enough for the butanol and hexanol monolayers to be fully reestablished at the surface of the acid.<sup>41</sup>

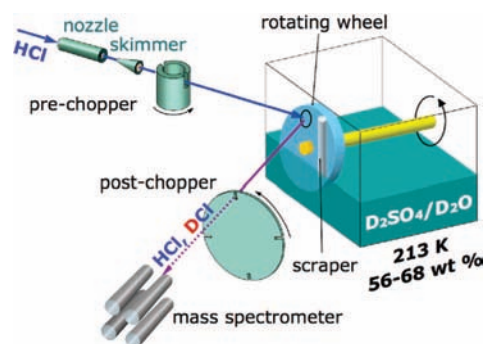


**FIGURE 2.** Apparatus and liquid reservoir for gas–liquid scattering experiments.

To map out the pathways depicted in Figure 1, we bombard the acid with HCl at selected collision energies ranging from near-thermal values of  $13 \text{ kJ mol}^{-1}$  ( $7RT_{\text{acid}}$ ) to hyperthermal energies of  $100 \text{ kJ mol}^{-1}$  ( $56RT_{\text{acid}}$ ).<sup>42</sup> These high-energy beams are often employed because they are more intense than thermal beams. As shown in Figure 2, the HCl beam is modulated by time-of-flight (TOF) wheels before or after colliding with the acid. The scattered and desorbing HCl and DCI molecules are then detected according to their arrival times at the mass spectrometer. The postchopper and prechopper experiments yield different information. In postchopper mode, the HCl beam strikes the acid continuously and the TOF spectra yield the relative intensities and velocities of all exiting HCl and  $H \rightarrow D$  exchanged DCI. In the prechopper mode, the incident HCl beam is pulsed instead, and the DCI and HCl arrival times are the sum of their gas-phase flight times and the time they spend dissolved in the acid. We can extract average solvation times between  $10^{-6}$  and  $10^{-2}$  s from these spectra, corresponding to diffusion depths between  $\sim 10$  and  $\sim 1000 \text{ \AA}$ .<sup>43</sup>

## Argon Atom Scattering: A Probe of Surfactant Segregation

Hyperthermal argon atom scattering, coupled with benchtop measurements of surface tension, provides a direct way to characterize the packing of butanol and hexanol at the surface of sulfuric acid in vacuum.<sup>34,41</sup> Figure 3a shows TOF spectra of  $90 \text{ kJ mol}^{-1}$  Ar scattering from 68 wt %  $D_2SO_4$  at 213 K containing 0–100 mM HexOD. The bimodal feature in each spectrum illustrates two distinct pathways that high-energy Ar atoms follow upon colliding with the surface. The narrow peak at early arrival times (high exit velocities) corresponds to Ar atoms that undergo direct inelastic scattering (IS), transferring on average 70% of their incident energy to the acid during one or a few collisions before recoiling away. The broader peak at later arrival times (lower exit velocities) is assigned to Ar atoms that fully dissipate their excess

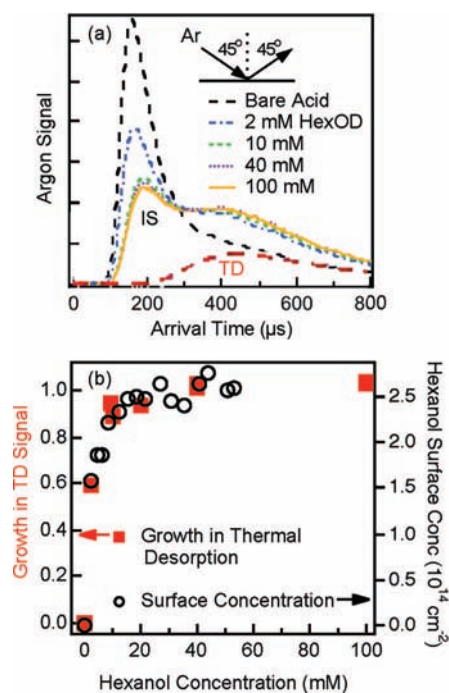


**FIGURE 3.** (a) Postchopper TOF spectra of high-energy Ar atoms scattering from pure and hexanol-doped sulfuric acid. "IS" and "TD" refer to direct inelastic scattering and thermal desorption. (b) The growth in TD signal matches the trend in hexanol surface concentration. Adapted from ref 34.

energy, become momentarily trapped at the surface, and then thermally desorb (TD). This TD component can be fit with a Maxwell–Boltzmann distribution at the acid temperature of 213 K (dashed red line).

Figure 3a shows that as hexanol is added to the acid, the IS component shrinks (fewer Ar atoms scatter directly) and shifts to later arrival times (the scattered Ar atoms exit with less kinetic energy).<sup>34</sup> Concurrently, the TD signal grows (more Ar atoms thermalize upon collision). These changes arise from the increased roughening of the surface and the reduced effective surface mass when hexyl chains coat the surface, which force the Ar atoms to undergo more bounces and dissipate more energy.<sup>40</sup> Because these Ar collisions probe only the outermost few layers,<sup>41</sup> Figure 3a demonstrates that hexanol segregates to the surface of the acid and significantly alters the initial encounter.

The Ar scattering patterns can be quantified by graphing the fractional increase in TD intensity,  $I_{TD}$ , relative to bare acid,  $(I_{TD}^{HexOD} - I_{TD}^{bare})/I_{TD}^{bare}$ , against bulk hexanol concentration. This fraction is plotted on the left side of Figure 3b, along with the surface concentration of hexanol on the right side, obtained from surface tension measurements.<sup>37,38</sup> The two plots show that the growth in Ar thermal desorption mirrors the change in surface concentration, each exhibiting Langmuir-like adsorption behavior. These matching trends, found in all of our stud-

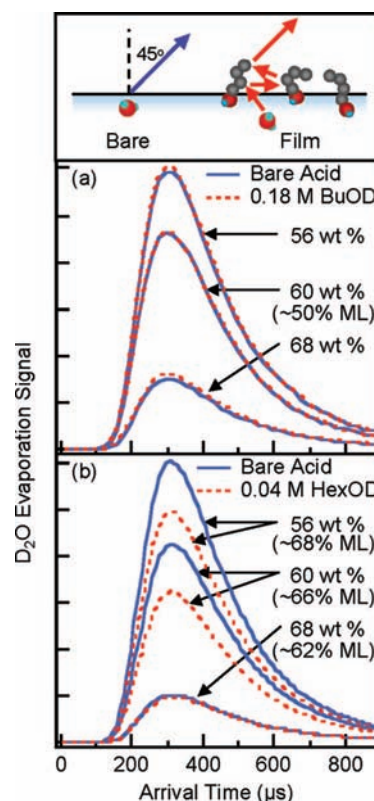


**FIGURE 4.** Water evaporation from sulfuric acid containing (a) butanol and (b) hexanol. The differences in TOF spectra show that butanol does not impede evaporation while hexanol slightly suppresses it. % ML is the fractional monolayer coverage. Adapted from refs 34 and 41.

ies, provide evidence that the hexanol surface concentration is similar when the monolayer is prepared on a continuously renewed, vertical acid film in vacuum and on a static, horizontal acid sample in air.

## Water Evaporation through Surfactant Films on Sulfuric Acid

Water evaporation through surfactants has been studied extensively in efforts to reduce water loss from reservoirs.<sup>2,25</sup> Conventional measurements carried out in air cannot easily be employed for short-chain surfactants, however, because the monolayer imposes a smaller resistance to gas transport than does the stagnant air layer above the sample.<sup>16</sup> Alternatively, vacuum-based experiments enable direct comparisons of the D<sub>2</sub>O evaporation rates from the pure and alcohol-doped acids.<sup>34,41</sup> Figure 4a compares TOF spectra of D<sub>2</sub>O evaporating from 56, 60, and 68 wt % D<sub>2</sub>SO<sub>4</sub> containing 0 and 0.18 M BuOD. The 0.18 M BuOD solutions generate butanol films with a surface concentration equal to ~50% of a compact monolayer on 60 wt % D<sub>2</sub>SO<sub>4</sub>, with values slightly higher and lower on 56 and 68 wt % acid, respectively.<sup>38</sup> In every case, the spectra for bare and butanol-doped acids are identical in

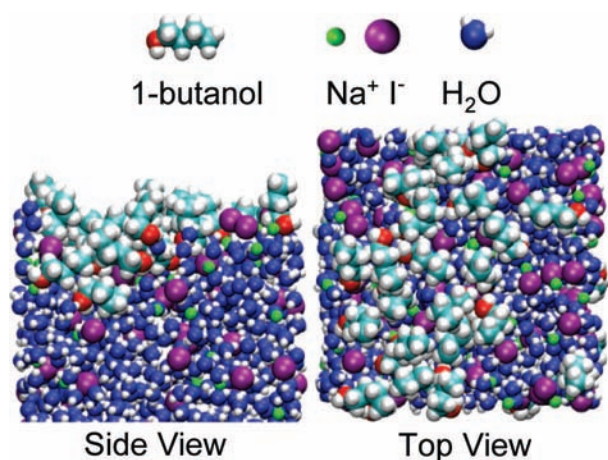


**FIGURE 5.** Top and side views of a simulation of a 56% butanol monolayer on the surface of an aqueous 5 M NaI solution. Adapted from ref 44 with permission.

shape and intensity, implying that the butyl films are fully permeable to  $D_2O$  molecules.

Why do butanol films have no effect on water evaporation? Figure 5 provides a hint. The snapshots depict molecular dynamics simulations of butanol at 56% coverage on top of an aqueous 5 M NaI solution at 298 K.<sup>44</sup> The side and top views show that the butanol molecules are loosely bundled and neither well-ordered nor evenly distributed. These simulations suggest that water molecules can readily move through fluctuating gaps between the chains. We imagine that  $D_2O$  molecules occasionally jump from the subsurface acid into the butyl film, dissolving back into the acid much more often than they desorb. In this limit,  $D_2O$  becomes equilibrated between the acid and film regions, saturating the film, and water evaporation would not be affected by small barriers in transport through the porous film itself.<sup>41</sup>

We can also view this process from the perspective of water molecules impinging on the butyl-coated acid. The unimpeded evaporation of water implies that, at equilibrium, the condensation of water must also be unaltered by the butanol films.<sup>41</sup> Figure 5 suggests that the permeation of impinging  $D_2O$  molecules through the butyl film is enforced by its porosity and by attractive forces between  $D_2O$  and the alkyl chains and OD head groups, which at low temperatures make it difficult for the  $D_2O$  to escape back into the gas phase before entering the acid. This inference agrees with molecular dynamics simulations, which predict that a methanol monolayer does not impede the entry of methanol into water at 273 K.<sup>45</sup>

Figure 4b indicates that the addition of hexanol, just two  $CH_2$  groups longer, destroys the invisibility of the butyl chains. Hexanol films impede water evaporation by  $\sim 20\%$  on 56 and 60 wt %  $D_2SO_4$ . The film does not alter water transport on 68 wt % acid, however, most likely because the greater fraction

of surface  $HexOD_2^+$  species at higher acid concentration leads to greater charge repulsion and looser chain–chain packing.

## Surfactant Control of HCl Uptake into Sulfuric Acid

The unimpeded evaporation of water through the butanol films led us to expect that HCl would also readily penetrate through the butyl chains. To our surprise, we found that butanol films actually enhance HCl uptake. The entry probability of HCl into the bare and surfactant-coated acids can be determined by measuring the fraction of thermalized HCl molecules that are converted into DCI after contact with the  $D_2SO_4/D_2O$  solution. Experiments using the prechopper TOF wheel indicate that HCl molecules that thermalize on the bare or film-coated acid and then desorb as intact HCl spend less than  $10^{-6}$  s in the acid, our shortest measurable time.<sup>43</sup> This upper limit corresponds to an average diffusion depth of less than 10 Å and likely implies that these HCl molecules thermalize on the surface and are then propelled back into the gas phase before they dissociate. In contrast, HCl molecules that are converted into DCI spend relatively long times in the acid ( $10^{-5}$  to  $10^{-2}$  s average residence times, depending on acid concentration<sup>46</sup>), most likely solvated as  $Cl^-$  and  $D^+/H^+$  and possibly as  $ClSO_3^-$ .<sup>47</sup> These observations imply that the  $H \rightarrow D$  exchange fraction,  $f_{exch}$ , equals the fraction of thermalized molecules that enter and dissolve into the acid and become available to react with other solute species.

Further experiments show that  $f_{exch}$  is independent of HCl collision energy from 100 to 13 kJ mol<sup>-1</sup>.<sup>34,42,43</sup> This invariance implies that HCl entry involves two steps: thermalization of the impinging HCl molecule at the surface, in which it loses memory of its initial trajectory and collision energy, and then entry of the thermalized HCl into the acid as molecular HCl or as  $Cl^-$  and  $H^+/D^+$  after dissociating at the surface. Because the trapping probability,  $p_{trap}$ , approaches 1 at thermal collision energies,  $f_{exch} = p_{enter}/p_{trap}$  is equal to the entry probability,  $p_{enter}$ , itself under thermal collision conditions. We therefore refer to  $f_{exch}$  and HCl entry probability interchangeably.

The parameter  $f_{exch}$  is measured from the data in Figure 6a,b, which shows TOF spectra of HCl and DCI exiting from bare 60 wt %  $D_2SO_4$  at 213 K following collisions of 100 kJ mol<sup>-1</sup> HCl. The HCl spectrum is composed of HCl molecules that scatter directly (IS) and those that thermalize and then desorb (TD). The DCI spectrum shows no evidence of directly scattered DCI, indicating that  $H \rightarrow D$  exchange occurs only after HCl is trapped at the surface. All HCl and DCI molecules

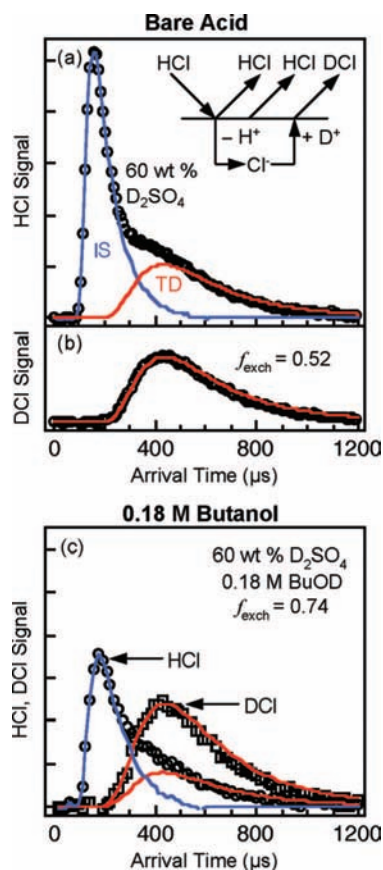


**FIGURE 6.** Postchopper TOF spectra of (a) HCl and (b) H → D exchanged DCI following collisions of HCl with 60 wt %  $D_2SO_4$  and (c) analogous spectra using 60 wt %  $D_2SO_4$  doped with 0.18 M butanol. The IS and TD channels are fit with blue and red curves, respectively. Note that  $f_{\text{exch}}$  increases upon adding butanol. Adapted from ref 42.

desorb from solution during the experiment, and  $f_{\text{exch}}$  is calculated from the magnitudes of the TOF signals.

The measured exchange fraction extracted from Figure 6a,b is  $0.52 \pm 0.02$  for collisions of HCl with bare 60 wt %  $D_2SO_4$ ; half of the thermalized HCl molecules undergo H → D exchange and then desorb as DCI, while the remaining HCl desorb before exchange. As shown later in Figure 7b, this entry probability increases steadily as the bare acid is diluted with water, rising from 0.1 in 70 wt %  $D_2SO_4$  to nearly 0.8 in 53 wt %  $D_2SO_4$ .<sup>46</sup> This trend implies that as the acid is diluted with water, more  $D_2O$  molecules become available in the interfacial region to act as hydrogen bonding and protonation sites for adsorbed HCl molecules, which then dissociate and dissolve in the acid.<sup>43</sup>

The effects of doping the acid with 0.18 M BuOD are displayed in Figure 6c.<sup>42</sup> Just as in argon atom scattering, fewer HCl molecules scatter directly from the butanol-covered acid and more HCl molecules thermalize upon collision. More importantly, the desorption of H → D exchanged DCI is nearly

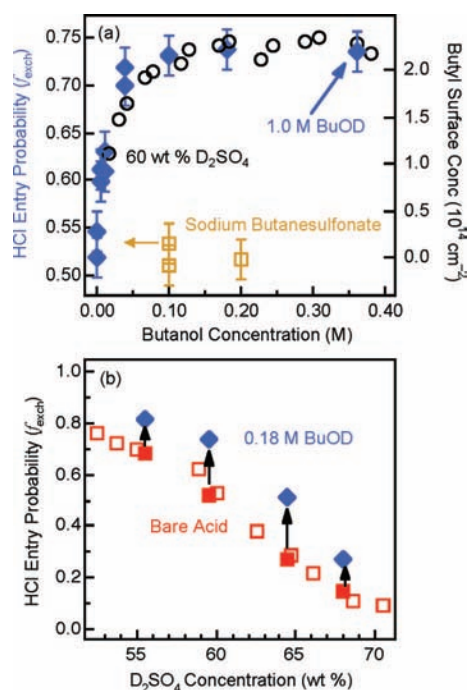


**FIGURE 7.** (a) H → D exchange fractions at 213 K ( $\blacklozenge$ ) and butanol surface concentrations at 295 K ( $\circ$ ) for 0–0.4 M butanol in 60 wt %  $D_2SO_4$  and (b) changes in HCl entry probability for 56–68 wt %  $D_2SO_4$  doped with 0.18 M butanol. Adapted from ref 42.

three times as strong as HCl desorption, indicating that  $f_{\text{exch}}$  rises from 0.52 to 0.74. The addition of BuOD enhances HCl entry into the acid!

Why do butanol molecules catalyze HCl uptake? Figure 7a summarizes our  $f_{\text{exch}}$  measurements for HCl molecules colliding with 60 wt %  $D_2SO_4$  containing 0–1 M BuOD.<sup>42</sup> The exchange fractions mirror the trend in butanol surface coverage, both increasing sharply at low butanol concentrations before approaching an asymptotic value characteristic of a Langmuir adsorption curve. This trend indicates that the increase in  $f_{\text{exch}}$  is caused by butyl species at the surface rather than in the bulk. When butanol is replaced by another butyl-based surfactant, sodium butanesulfonate ( $CH_3CH_2CH_2CH_2-SO_3^- Na^+$ ), no increase in H → D exchange is observed despite surface coverage comparable to that of butanol.<sup>38</sup> This molecule was chosen because the C–S linkage eliminates the basic oxygen atom in butanol and the  $SO_3^-$  group is not readily protonated by HCl. The unchanging  $f_{\text{exch}}$  values for sodium butanesulfonate demonstrate that the alcohol OD group is necessary for enhancing HCl uptake. This observation suggests that butanol enhances entry because the OD groups of surface BuOD molecules provide extra interfacial hydrogen bonding and protonation sites that assist HCl dissociation via  $BuOD + HCl \rightarrow BuODH^+ + Cl^-$ , just as interfacial water molecules supplied by dilution enhance  $DOD + HCl \rightarrow DODH^+ + Cl^-$ . HCl molecules can therefore be “teased” into

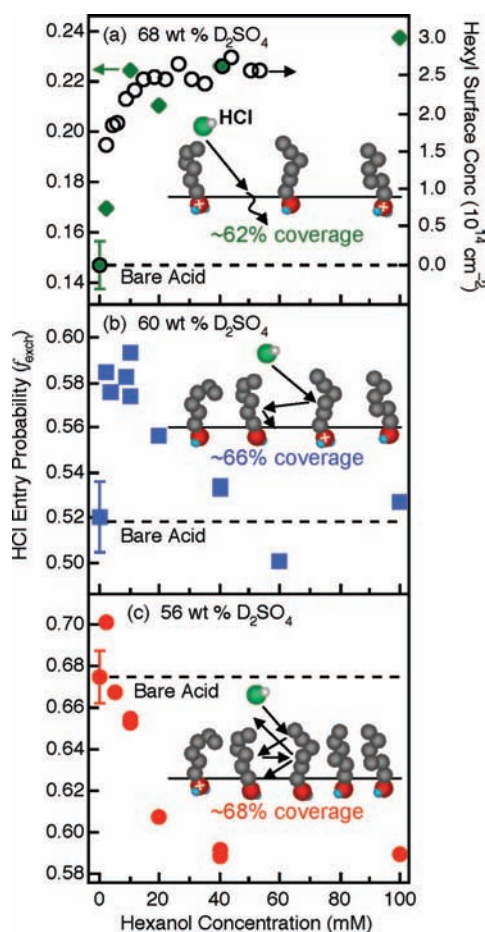


**FIGURE 8.** HCl entry probability ( $f_{\text{exch}}$ ) versus hexanol concentration in 56, 60, and 68 wt %  $\text{D}_2\text{SO}_4$  at 213 K.  $f_{\text{exch}}$  varies with hexanol surface coverage and with acid concentration. Adapted from ref 34.

the acid by coating the surface with a porous but protonatable surfactant.

Butanol catalyzes HCl uptake over a wide range of acid concentrations, as displayed in Figure 7b; in no instance does butanol impede HCl entry. This is not the case for hexanol. The Langmuir-like increase in  $\text{H} \rightarrow \text{D}$  exchange is observed for hexanol coatings on 68 wt %  $\text{D}_2\text{SO}_4$ , as shown in Figure 8a, where the highest hexyl coverage is  $\sim 62\%$  of maximum packing.<sup>34</sup> At lower acid concentrations, however, the hexanol films become slightly more compact and impede entry. Figure 8b shows that on 60 wt %  $\text{D}_2\text{SO}_4$ ,  $f_{\text{exch}}$  rises at low hexanol concentrations and then falls back to the bare acid value as the hexyl chains pack just 4% more tightly than on 68 wt % acid. The chains pack even more closely on 56 wt %  $\text{D}_2\text{SO}_4$ , reaching a maximum of  $\sim 68\%$  full coverage and causing  $f_{\text{exch}}$  to drop  $\sim 13\%$  lower than the bare value, as shown in Figure 8c.

This marks our first observation that a soluble surfactant can actually impede the entry of HCl into sulfuric acid.

## Uptake of Trifluoroethanol and Hydrolysis of $\text{N}_2\text{O}_5$

The HCl experiments demonstrate that the resistance imposed by an alcohol film depends on chain length and acid concentration. This resistance also depends on the identity of the permeating gas. The entry of the basic molecule  $\text{CF}_3\text{CH}_2\text{OH}$ , like the evaporation of  $\text{D}_2\text{O}$ , is essentially unimpeded by butyl or hexyl species under all conditions in Figures 6–8.<sup>34,42</sup> Because  $\text{CF}_3\text{CH}_2\text{OH}$  is nearly four times larger than  $\text{D}_2\text{O}$ , size alone does not appear to control permeation. The unimpeded entry of  $\text{CF}_3\text{CH}_2\text{OH}$  may be due to its high polarizability, which enhances gas–chain attractions, and to facile protonation of  $\text{CF}_3\text{CH}_2\text{OH}$  by  $\text{D}_3\text{O}^+$  and  $\text{D}_2\text{SO}_4$  at the interface or intercalated within the chains. Hydrogen bonding between  $\text{CF}_3\text{CH}_2\text{OH}$  and interfacial alcohol OD groups may also momentarily anchor the molecule within the film and draw it into the acid.

In contrast, Figure 9a shows that the hydrolysis of  $\text{N}_2\text{O}_5$  is reduced from 0.15 to 0.06 by hexanol films on 72 wt %  $\text{H}_2\text{SO}_4$  under the same conditions where the entry of HCl is enhanced.<sup>48</sup> Figure 9b reveals that the reductions increase linearly with hexanol surface coverage, implying a constant “blocking power” for each added hexanol molecule (just as HCl entry increases linearly with butanol surface coverage, implying that each added butanol molecule provides one additional dissociation site). Panel b also shows that butanol films impede hydrolysis but to a lesser extent (from 0.15 to 0.10 at maximum coverage).  $\text{N}_2\text{O}_5$  is similar in volume to  $\text{CF}_3\text{CH}_2\text{OH}$  but lacks OH groups that can hydrogen bond to interfacial acid or alcohol species, and in this case, the large size of  $\text{N}_2\text{O}_5$  may create barriers to transport. Alternatively, hydrolysis may be inhibited because the butanol and hexanol OH groups crowd the surface region,<sup>48</sup> reducing the availability of near-interfacial  $\text{H}_3\text{O}^+$  and  $\text{H}_2\text{O}$  that participate in the conversion of  $\text{N}_2\text{O}_5$  into  $\text{HNO}_3$ .<sup>21,30</sup>

## Three Faces of a Soluble Surfactant

Our expectation that even a porous film would reduce gas uptake has broadened into a multifaceted picture of short-chain surfactants. The experiments illustrate three classes of permeating molecules: acidic gases such as HCl, whose entry into the acid is assisted by surfactant OH head groups that provide extra dissociation sites; basic gases such as  $\text{H}_2\text{O}$  and  $\text{CF}_3\text{CH}_2\text{OH}$ , whose unimpeded transport may be enforced by attractive gas–chain interactions, interfacial hydrogen bond-

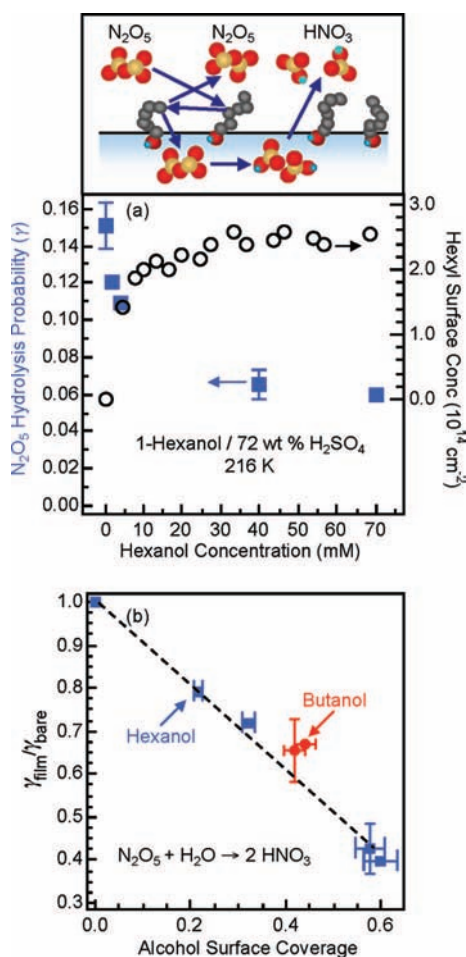


**FIGURE 9.** (a)  $\text{N}_2\text{O}_5$  hydrolysis probability,  $\gamma$ , for 0 to 70 mM hexanol in 72 wt %  $\text{H}_2\text{SO}_4$  at 216 K and (b) ratio of hydrolysis probabilities,  $\gamma_{\text{film}}/\gamma_{\text{bare}}$ , versus hexanol and butanol surface coverage. Adapted from ref 48.

ing, and protonation by  $\text{H}_3\text{O}^+$  or  $\text{H}_2\text{SO}_4$ ; and nonprotic gases such as  $\text{N}_2\text{O}_5$ , whose large size may limit transport and whose reaction with subphase water may be interrupted because the surfactant reduces access to interfacial  $\text{H}_3\text{O}^+$  and  $\text{H}_2\text{O}$ . Ongoing experiments indicate that the uptake of HCl is also assisted at low concentrations of pentanoic acid, another soluble surfactant, implying that HCl can protonate both COOH and OH groups at the surface of sulfuric acid.

From an atmospheric perspective, our studies show that short-chain surfactants do not pack tightly enough to limit solute–solute reactions such as  $\text{HCl}(\text{g}) + \text{HOBr}(\text{aq}) \rightarrow \text{BrCl}(\text{g}) + \text{H}_2\text{O}$ . While hexanol impedes HCl entry by  $\sim 13\%$  in 56 wt %  $\text{D}_2\text{SO}_4$ , the bulk-phase probability for reaction is only  $10^{-4}$ , and this low value constrains the overall rate.<sup>19,20</sup> Additionally, butanol and hexanol do not pack tightly enough to limit water transport at high acid concentrations, implying that small surfactants are unlikely to alter the growth or shrinkage of midlatitude sulfuric acid aerosols. The transition from

a barrierless butanol layer to a slightly impermeable hexanol film at lower acid concentrations suggests that longer surfactants can alter water transport. Even butanol, however, suppresses the hydrolysis of  $\text{N}_2\text{O}_5$  on 72 wt %  $\text{H}_2\text{SO}_4$  at 213 K. This solute–solvent reaction is responsible for denitrifying the troposphere by  $\sim 50\%$  and reducing ozone concentrations by  $\sim 10\%$ .<sup>49</sup> The 30% and 60% reductions in hydrolysis imposed by butanol and hexanol films would be important, however, only if enough surfactant is present in the droplets to cover a significant fraction of the surface.

These studies also raise questions from a microscopic viewpoint about the interconnected motions of the permeating gas, surfactant, and acid species. The trajectories of HCl molecules striking bare acid must be different from HCl molecules that move through the film before reaching the acid. Do the changes in  $f_{\text{exch}}$  upon adding butanol or hexanol reflect two competing factors, one in which neighboring alkyl chains interrupt HCl transport and the other in which the chains provide a cage for repeated collisions between HCl and  $\text{D}_2\text{O}$  or ROD that enhance HCl dissociation? This type of competition is indeed observed in simulations of  $\text{O}_3$  molecules moving through the fluctuating butyl chains depicted in Figure 5.<sup>44,50</sup> We hope that experiments and simulations together can continue to address similar questions and reveal new insights into the pathways by which surfactants on sulfuric acid and other aqueous solutions control gas transport and interfacial reactions.

*We gratefully acknowledge the Air Force Office of Scientific Research, the Camille and Henry Dreyfus Foundation, and the Vilas Foundation for their support. We also thank our co-workers John Morris, Peter Behr, Melissa Antman, Jennifer Lawrence, Samuel Glass, Ryan Torn, James Krier, and Alexis Johnson and thank Raffaella D’Auria and Doug Tobias for sharing their simulations.*

#### BIOGRAPHICAL INFORMATION

**Seong-Chan Park** received his Ph.D. degree from POSTECH, South Korea, under the direction of Heon Kang. He was a Dreyfus Environmental Chemistry Fellow with Gilbert Nathanson and is currently a research scientist at Samsung Electro-Mechanics.

**Daniel Burden** received his B.S. degree from the University of Maryland and is currently a graduate student with Gilbert Nathanson.

**Gilbert Nathanson** received his Ph.D. degree under the direction of Gary McClelland at Harvard University. He was a Miller Postdoctoral Fellow with Yuan Lee at the University of California, Berkeley, before moving to Wisconsin in 1988.



## REFERENCES

- Boys, C. V. *Soap Bubbles*; Dover: New York, 1959.
- Gaines, G. L. *Insoluble Monolayers at Liquid-Gas Interfaces*; Interscience: New York, 1966; Chapter 4.
- Moore, F. G.; Richmond, G. L. Integration or Segregation: How Do Molecules Behave at Oil/Water Interfaces. *Acc. Chem. Res.* **2008**, *41*, 739–748.
- Carlsaw, K. S.; Peter, T.; Clegg, S. L. Modeling the Composition of Liquid Stratospheric Aerosols. *Rev. Geophys.* **1997**, *35*, 125–154.
- Hanson, D. R.; Ravishankara, A. R.; Solomon, S. Heterogeneous Reactions in Sulfuric Acid Aerosols - A Framework for Model Calculations. *J. Geophys. Res. Atmos.* **1994**, *99*, 3615–3629.
- Jacob, D. J. Heterogeneous Chemistry and Tropospheric Ozone. *Atmos. Environ.* **2000**, *34*, 2131–2159.
- Finlayson-Pitts, B. J.; Pitts, J. N. *Chemistry of the Upper and Lower Atmosphere*; Academic Press: New York, 2000; Chapters 7.D, 9.C, and 12.C.
- Hanson, D. R.; Lovejoy, E. R. Heterogeneous Reactions in Liquid Sulfuric Acid: HOCl + HCl as a Model System. *J. Phys. Chem.* **1996**, *100*, 6397–6405.
- Bianco, R.; Hynes, J. T. Heterogeneous Reactions Important in Atmospheric Ozone Depletion: A Theoretical Perspective. *Acc. Chem. Res.* **2006**, *39*, 159–165.
- Solomon, S. Stratospheric Ozone Depletion: A Review of Concepts and History. *Rev. Geophys.* **1999**, *37*, 275–316.
- Murphy, D. M.; Thomson, D. S.; Mahoney, T. M. J. In Situ Measurements of Organics, Meteoritic Material, Mercury, and Other Elements in Aerosols at 5 to 19 Kilometers. *Science* **1998**, *282*, 1664–1669.
- Donaldson, D. J.; Vaida, V. The Influence of Organic Films at the Air–Aqueous Boundary on Atmospheric Processes. *Chem. Rev.* **2006**, *106*, 1445–1461.
- Gill, P. S.; Graedel, T. E.; Weschler, C. J. Organic Films on Atmospheric Aerosol Particles, Fog Droplets, Cloud Droplets, Raindrops, and Snowflakes. *Rev. Geophys. Space Phys.* **1983**, *21*, 903–920.
- Rudich, Y. Laboratory Perspectives on the Chemical Transformations of Organic Matter in Atmospheric Particles. *Chem. Rev.* **2003**, *103*, 5097–5124.
- Archer, R. J.; La Mer, V. K. The Rate of Evaporation of Water through Fatty Acid Monolayers. *J. Phys. Chem.* **1955**, *59*, 200–208.
- Barnes, G. T. Permeation through Monolayers. *Colloids Surf. A* **1997**, *126*, 149–158.
- Farajzadeh, R.; Krastev, R.; Zitha, P. L. J. Foam Film Permeability: Theory and Experiment. *Adv. Colloid Interface Sci.* **2008**, *137*, 27–44.
- Reactive species such as OH may also react with the surfactant. See: Ellison, G. B.; Tuck, A. F.; Vaida, V. Atmospheric Processing of Organic Aerosols. *J. Geophys. Res. Atmos.* **1999**, *104*, 11633–11641.
- Waschewsky, G. C. G.; Abbatt, J. P. D. HOBr in Sulfuric Acid Solutions: Solubility and Reaction as a Function of Temperature and Concentration. *J. Phys. Chem. A* **1999**, *103*, 5312–5320.
- Hanson, D. R. Reactivity of BrONO<sub>2</sub> and HOBr on Sulfuric Acid Solutions at Low Temperatures. *J. Geophys. Res. Atmos.* **2003**, *108*, 4239.
- Robinson, G. N.; Worsnop, D. R.; Jayne, J. T.; Kolb, C. E.; Davidovits, P. Heterogeneous Uptake of ClONO<sub>2</sub> and N<sub>2</sub>O<sub>5</sub> by Sulfuric Acid Solutions. *J. Geophys. Res. Atmos.* **1997**, *102*, 3583–3601.
- Brown, S. S.; Ryerson, T. B.; Wollny, A. G.; Brock, C. A.; Peltier, R.; Sullivan, A. P.; Weber, R. J.; Dube, W. P.; Trainer, M.; Meagher, J. F.; Fehsenfeld, F. C.; Ravishankara, A. R. Variability in Nocturnal Nitrogen Oxide Processing and its Role in Regional Air Quality. *Science* **2006**, *311*, 67–70.
- Singh, H.; Chen, Y.; Staudt, A.; Jacob, D.; Blake, D.; Heikes, B.; Snow, J. Evidence from the Pacific Troposphere for Large Global Sources of Oxygenated Organic Compounds. *Nature* **2001**, *410*, 1078–1081.
- Penner, J. E.; Lister, D. H.; Griggs, D. J.; Dokken, D. J.; McFarland, M. Aviation and the Global Atmosphere; Report of the Intergovernmental Panel on Climate Change, 2001; www.grida.no/climate/ipcc/aviation/index.htm.
- Barnes, G. T. The Potential for Monolayers to Reduce the Evaporation of Water from Large Water Storages. *Agric. Water Manag.* **2008**, *95*, 339–353.
- For reviews, see refs 7, 12, 17, and 44 and Chuang, P. Y. Measurement of the Timescale of Hygroscopic Growth of Atmospheric Aerosols. *J. Geophys. Res. Atmos.* **2003**, *108*, 4282.
- Cosman, L. M.; Knopf, D. A.; Bertram, A. K. N<sub>2</sub>O<sub>5</sub> Reactive Uptake on Aqueous Sulfuric Acid Solutions Coated with Branched and Straight-Chain Insoluble Organic Surfactants. *J. Phys. Chem. A* **2008**, *112*, 2386–2396.
- Gilman, J. B.; Vaida, V. Permeability of Acetic Acid through Organic Films at the Air–Aqueous Interface. *J. Phys. Chem. A* **2006**, *110*, 7581–7587.
- Cosman, L. M.; Bertram, A. K. Reactive Uptake of N<sub>2</sub>O<sub>5</sub> on Aqueous H<sub>2</sub>SO<sub>4</sub> Solutions Coated with 1-Component and 2-Component Monolayers. *J. Phys. Chem. A* **2008**, *112*, 4625–4635.
- Thornton, J. A.; Abbatt, J. P. D. N<sub>2</sub>O<sub>5</sub> Reaction on Submicron Sea Salt Aerosol: Kinetics, Products, and the Effect of Surface Active Organics. *J. Phys. Chem. A* **2005**, *109*, 10004–10012.
- McNeill, V. F.; Patterson, J.; Wolfe, G. M.; Thornton, J. A. The effect of varying levels of surfactant on the reactive uptake of N<sub>2</sub>O<sub>5</sub> to aqueous aerosol. *Atmos. Chem. Phys.* **2006**, *6*, 1635–1644.
- Clifford, D.; Bartels-Rausch, T.; Donaldson, D. J. Suppression of Aqueous Surface Hydrolysis by Monolayers of Short Chain Organic Amphiphiles. *Phys. Chem. Chem. Phys.* **2007**, *9*, 1362–1369.
- Mmerekhi, B. T.; Chaudhuri, S. R.; Donaldson, D. J. Enhanced Uptake of PAHs by Organic-Coated Aqueous Surfaces. *J. Phys. Chem. A* **2003**, *107*, 2264–2269.
- Glass, S. V.; Park, S.-C.; Nathanson, G. M. Evaporation of Water and Uptake of HCl and HBr through Hexanol Films at the Surface of Supercooled Sulfuric Acid. *J. Phys. Chem. A* **2006**, *110*, 7593–7601.
- Minerath, E. C.; Casale, M. T.; Elrod, M. J. Kinetics Feasibility Study of Alcohol Sulfate Esterification Reactions in Tropospheric Aerosols. *Environ. Sci. Technol.* **2008**, *42*, 4410–4415.
- Lee, D. G.; Cameron, R. The Basicity of Ethanol. An Acidity Function for Alcohols. *J. Am. Chem. Soc.* **1971**, *93*, 4724–4728.
- Torn, R. D.; Nathanson, G. M. Surface Tension and Surface Segregation of n-Butanol in Sulfuric Acid. *J. Phys. Chem. B* **2002**, *106*, 8064–8069.
- Krier, J. M.; Nathanson, G. M. Manuscript in preparation.
- Van Loon, L. L.; Minor, R. N.; Allen, H. C. Structure of Butanol and Hexanol at Aqueous Ammonium Bisulfate, and Sulfuric Acid Solution Surfaces Investigated by Vibrational Sum Frequency Generation Spectroscopy. *J. Phys. Chem. A* **2007**, *111*, 7338–7346.
- Nathanson, G. M. Molecular Beam Studies of Gas-Liquid Interfaces. *Annu. Rev. Phys. Chem.* **2004**, *55*, 231–255.
- Lawrence, J. R.; Glass, S. V.; Nathanson, G. M. Evaporation of Water through Butanol Films at the Surface of Supercooled Sulfuric Acid. *J. Phys. Chem. A* **2005**, *109*, 7449–7457.
- Lawrence, J. R.; Glass, S. V.; Park, S.-C.; Nathanson, G. M. Surfactant Control of Gas Uptake: Effect of Butanol Films on HCl and HBr Entry into Supercooled Sulfuric Acid. *J. Phys. Chem. A* **2005**, *109*, 7458–7465.
- Morris, J. M.; Behr, P.; Antman, M. D.; Ringeisen, B. R.; Splan, J.; Nathanson, G. M. Molecular Beam Scattering from Supercooled Sulfuric Acid: Collisions of HCl, HBr, and HNO<sub>3</sub> with 70 wt % D<sub>2</sub>SO<sub>4</sub>. *J. Phys. Chem. A* **2000**, *104*, 6738–6751.
- Krisch, M. J.; D'Auria, R.; Brown, M. A.; Tobias, D. J.; Hemminger, J. C.; Ammann, M.; Starr, D. E.; Bluhm, H. The Effect of an Organic Surfactant on the Liquid–Vapor Interface of an Electrolyte Solution. *J. Phys. Chem. C* **2007**, *111*, 13497–13509.
- Morita, A. Molecular Dynamics Study of Mass Accommodation of Methanol at Liquid–Vapor Interfaces of Methanol/Water Binary Solutions of Various Concentrations. *Chem. Phys. Lett.* **2003**, *375*, 1–8.
- Behr, P.; Morris, J. R.; Antman, M. D.; Ringeisen, B. R.; Splan, J. R.; Nathanson, G. M. Reaction and Desorption of HCl and HBr Following Collisions with Supercooled Sulfuric Acid. *Geophys. Res. Lett.* **2001**, *28*, 1961–1964.
- Robinson, G. N.; Worsnop, D. R.; Jayne, J. T.; Kolb, C. E.; Swartz, E.; Davidovits, P. Heterogeneous Uptake of HCl by Sulfuric Acid Solutions. *J. Geophys. Res. Atmos.* **1998**, *103*, 25371–25381.
- Park, S.-C.; Burden, D. K.; Nathanson, G. M. The Inhibition of N<sub>2</sub>O<sub>5</sub> Hydrolysis in Sulfuric Acid by 1-Butanol and 1-Hexanol Surfactant Coatings. *J. Phys. Chem. A* **2007**, *111*, 2921–2929.
- Dentener, F. J.; Crutzen, P. J. Reaction of N<sub>2</sub>O<sub>5</sub> On Tropospheric Aerosols - Impact on the Global Distributions of NO<sub>x</sub>, O<sub>3</sub>, and OH. *J. Geophys. Res. Atmos.* **1993**, *98*, 7149–7163.
- D'Auria, R.; Tobias, D. J. Manuscript in preparation.